Environmental Engineering and Management Journal January 2019, Vol.18, No. 1, 31-39
http://www.eemj.icpm.tuiasi.ro/; http://www.eemj.eu

"Gheorghe Asachi" Technical University of Iasi, Romania

COMPARISON OF SOURCES AND SPATIAL DISTRIBUTION OF HEAVY METALS AT TWO PERI-URBAN AREAS IN SOUTHWEST SHENYANG, CHINA

Jin Wu[1], Yanguo Teng[2*], Binbin Wu[2], Jie Su[2], Jinsheng Wang[2]

[1]*College of Architecture and Civil Engineering, Beijing University of Technology, Beijing 100124, China*
[2]*College of Water Sciences, Beijing Normal University, 100875, China*

Abstract

To investigate the sources and spatial distribution of heavy metals in soil, samples were collected at two scales from the alluvial plains of Shenyang, China. Statistical analysis at small scale showed average concentrations of Cu, Pb, Zn, Ni, Cr and As of 36.76, 33.33, 100.06, 37.98, 91.26, and 7.99 mg/kg, respectively. Corresponding large-scale concentrations were 34.11, 46.38, 82.44, 32.51, 83.77, and 24.06 mg/kg. At both scales, Ni and Cr were mainly controlled by parent materials and Pb by anthropogenic activities. The main sources of Cu, Zn and As varied with scale. To describe the spatial structure of heavy metals, geostatistical analysis and geographic information systems were used to visualize and compare levels in different areas at both scales. The samples at small scales were located in the region of strong variation at large scale, indicating that the sampling strategy is appropriate for obtaining more reliable interpolation results. Health risk assessment based on 95th percentile concentrations of total elemental concentrations indicated that noncancer effect and cancer effect of children and adults were acceptable at the two different scales.

Keywords: heavy metals, multivariate statistics, risk assessment, spatial distribution

Received: December, 2013; Revised final: April, 2015; Accepted: April, 2015; Published in final edited form: January, 2019

1. Introduction

Soil is a vital natural non-renewable resource at human timescales, and has key environmental, economic, and social functions (Vrščaj et al., 2008). With rapid development of urbanization and industrialization in recent years, increasing release of heavy metals into urban soil has become a public concern in China, not only because of ecological and human health risks, but also because of potentially great financial implications in terms of remediation costs and redevelopment issues (Huang et al., 2007; Li et al., 2017; Semenzin et al., 2007). High concentrations of heavy metal in surface soil can threaten human health via inhalation, ingestion and dermal contact absorption (Pal et al., 2018; Sun et al., 2010; Xie et al., 2011), and they affect air quality by generating airborne particles and dust (Chen et al., 1997; Cyrys et al., 2003; Gray et al., 2003). Heavy metals in deep soil may result in groundwater contamination (Camobreco et al., 1996; Richards et al., 1998). In addition, many metals are more mobile and available for uptake in soil with low pH, compared with neutral or alkaline soil (Matache et al., 2018; Wei and Yang, 2010). Heavy metals in urban soils mainly originate from natural background and anthropogenic contamination, and show great spatial variability.

There are numerous studies on the source and spatial distribution of heavy metal in soil, at different scales (e.g., mining areas, vegetable fields, industrial areas and metropolises) (Fu and Wei, 2012; Lin et al., 2010; Liu et al., 2006; Yu et al., 2017). In contrast, there have been few studies comparing differences of sources and spatial distribution of heavy metals at two

*Author to whom all correspondence should be addressed: e-mail: teng1974@163.com; Phone:+86 010 58802738; Fax: +86 010 58802738

scales (Huo et al., 2009; Liu et al., 2009; Sylla et al., 1995). The spatial structures of these metals in soil vary between large and small scales. Studies at large scales cannot fully describe sources and spatial variation, because long distances between samples may conceal or neglect some small-scale information (Chen et al., 2009). Researches at small scales often ignore spatial variation at large scales, which provide significant information for regional soil management. Therefore, it is essential to study the difference of sources and spatial variations between small and large scales.

Shenyang in Northeast China has been known for its excellent industrial system forms. It has a total area of 13000 km^2 and a population over 7.2 million. Previous studies have shown a clear accumulation of heavy metal in soil within typical districts of Shenyang. An investigation of 36 samples in seven districts indicated that 63.89%, 77.78%, 94.44%, and 100% of soil samples were moderately or heavily contaminated by Cd, Cu, Pb and Zn, respectively (Sun et al., 2010). In the Tiexi industrial district, kriging maps indicated highest concentrations of Cd, Cu, Pb, Zn and Hg were higher than their corresponding pollution thresholds in China (MEP, 1995) not only in industrial areas, but also their wide distributions in residential areas and parks (Li et al., 2013). However, soil contamination in peri-urban areas near industrial regions was often neglected. The peri-urban area in southeast Shenyang was a traditional base of foodstuffs and vegetables, and transitioned from a traditionally agriculture-based economy to an industrial one. The present study of a peri-urban area provides valuable information for helping decision makers to identify locations where remediation efforts should focus.

The primary objectives are: (1) to identify the pollution source of these metals using multivariate analysis; (2) to compare the difference of spatial distribution of the metals at two scales; (3) to estimate population health risk due to heavy metal exposure according to Hazard Indexes (HIs) and cancer risk.

2. Experimental

2.1. Sampling

In September and October 2011, sampling was done in southwest Shenyang, using a global positioning system (GPS) for geo-referencing each location (122°25′–123°48′ E, 41°11′–43°2′ N) (Fig. 1). A systematic sampling strategy was implemented to provide a sampling program for the entire area. In each sample site, agricultural topsoil (0~15 cm) in the farmland or abandoned farmland was collected, and each sample was controlled at 1~1.5 kg. Forty topsoil samples were randomly distributed at small scale, based on a 700 m×700 m grid. To avoid sampling of field paths, field ditches and other artificial buildings, some sampling points were selected around designated sampling nodes, and each grid had at least one sampling point. Forty topsoil samples along four cross-sections of the Hun River were collected at large scale. The main soil type was meadow brown soil, with a texture classification of loam. Food crops were mainly corn and vegetables. The samples were air-dried at room temperature, and sieved through a 2-mm polyethylene sieve to remove plant roots, large debris, and gravel-sized materials. The sieved soil samples were then ground with pestle and mortar until all particles passed through a 0.149-mm mesh.

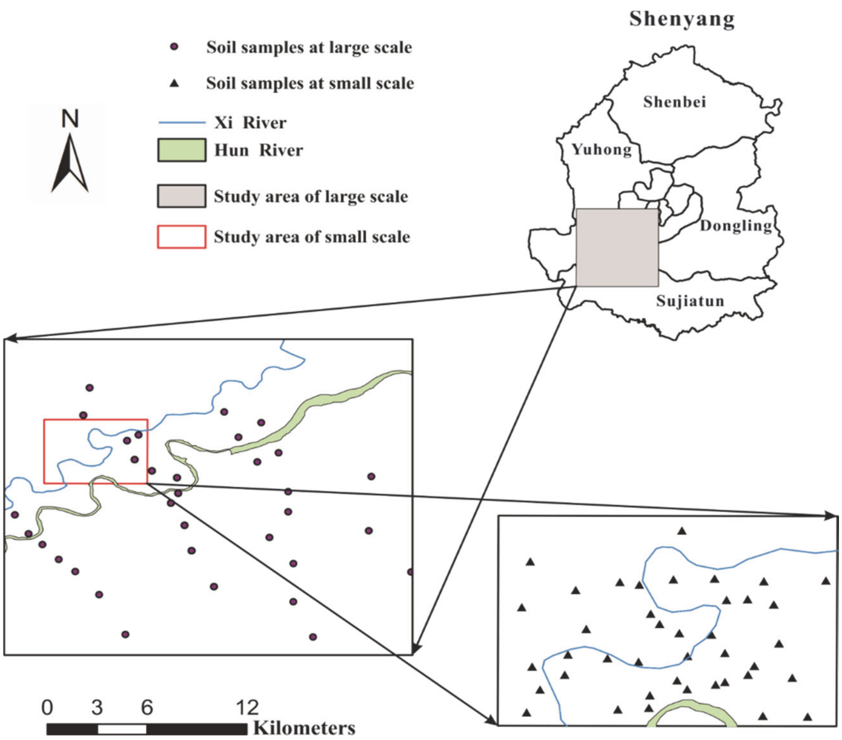

Fig. 1. The study area and the spatial pattern of soil samples

2.2. Chemical analysis

For content analysis of soil, Cu, Pb, Zn, Ni, Cr and As, soil samples were determined by acid digestion with a mixture of HNO_3-HF-$HClO_4$, followed by Inductively Coupled Plasma Atomic Emission Spectrometry for Cu, Pb, Zn, Ni, Cr and As. A blank reagent and standard reference material GSS-1 soil (China National Center for Standard Materials) were included for quality assurance and quality control (one blank and one standard from each 10 samples). Recoveries of samples spiked with standards between 95 and 105%.

2.3. Geostatistical methods

Geostatistics uses a (semi-)variogram to describe spatial structures based on theoretical regionalized variables, and its increasing use in environmental applications testifies to its utility and success (McGrath et al., 2004; Saito and Goovaerts, 2000). Semi-variance measures the mean variability between paired data values $Z(x)$ and $Z(x+h)$, as a function of their distance h. An experimental variogram fitted with a theoretical model gives information on the structure of the spatial variation. For discrete soil sampling sites, the function is estimated as (Eq. 1) (McGrath et al., 2004):

$$\gamma(h) = \frac{1}{2N(h)} \sum_{i=1}^{N(h)} \left[Z(x_i) - Z(x_i + h)\right]^2 \qquad (1)$$

where: $\gamma(h)$ is the semi-variance value at distance interval h; $N(h)$ is the number of sample pairs within h; and $Z(x_i+h)$ and $Z(x_i)$ are sample values at two points separated by h.

Inverse distance weighting (IDW) has been extensively used in soil investigation and pollution mapping (Tomczak, 1998; Xie et al., 2011). The interpolating function is (Eq. 2):

$$Z(x) = \frac{\sum_{i=1}^{n} Z_i d_i^{-u}}{\sum_{i=1}^{n} d_i^{-u}} \qquad (2)$$

where: $Z(x)$ is the predicted value at an interpolated point, Z_i is sample value in point i, d_i is the distance between point i and the prediction point, u is the weighting power that decides how the weight decreases as the distance increases, and n is the number of known points used in interpolation. Geostatistical analysis was done with GS+ (version 9). Interpolation mapping was conducted using IDW within ArcGIS 9.30 software.

2.4. Statistical analysis

Descriptive statistical analysis was performed for improved data understanding. Multivariate statistical analysis, including principal component analysis (PCA) and correlation matrix (CM) were done to identify the relationship among heavy metals in soil and their possible sources. Descriptive statistical parameters and multivariate statistics were obtained using commercial statistics software package SPSS (version 17).

2.5. Risk assessment model

According to the Exposure Factors Handbook (USEPA, 1997), the average daily dose (*ADD*) (mg/kg/day) of a pollutant via soil ingestion, dermal contact and inhalation as exposure pathways can be estimated using (Eqs. 3-5):

$$ADD_{ingest} = \frac{c \times IngR \times EF \times ED \times CF}{BW \times AT} \qquad (3)$$

$$ADD_{\mathrm{inh}} = \frac{\mathrm{c} \times SA \times AF_{\mathrm{soil}} \times ABS \times EF \times ED \times CF}{BW \times AT} \qquad (4)$$

$$ADD_{\mathrm{der}} = \frac{\mathrm{c} \times IngR \times EF \times ED \times CF}{PEF \times BW \times AT} \qquad (5)$$

For carcinogens, the lifetime average daily dose (*LADD*) used in the assessment of cancer risk has been calculated as a weighted average for each exposure route as shown in Eq. (6):

$$LADD_{\mathrm{inh}} = \frac{c \times EF}{PEF \times AT} \times \left(\frac{InhR \times ED_{adult}}{BW_{adult}} + \frac{InhR \times ED_{child}}{BW_{child}}\right) \qquad (6)$$

where: *C* (Concentration of the contaminant in soil, mg/kg) is considered to yield an estimate of the reasonable maximum exposure, which is the upper limit of the 95% confidence interval for the mean; *IngR*: ingestion rate, in this study, 200 mg/day for children ($IngR_{child}$) and 100 mg/day for adults ($IngR_{adult}$) (USEPA, 2001); *EF*: exposure frequency, in this study, 180 days/year; *ED*: exposure duration, in this study, 6 years for children (ED_{child}) and 24 years for adults (ED_{adult}) (USEPA, 2001); *BW*: average body weight; in this study, 15 kg for children (BW_{child}) and 60 kg for adults (BW_{adult}). *AT*: averaging time; for non-carcinogens, *ED*×365 days, *CF*: conversion factor, 1×10^{-6} kg/mg; *SA*: exposed skin area; in this study, 2800cm^2 for children (SA_{child}) and 5700cm^2 for adults (SA_{adult}) (USEPA, 2001); AF_{soil}: Skin adherence factor for soil, in this study, 0.2 mg/ cm^2 for children and adults. *ABS*: dermal absorption factor (unitless), in this study, 0.001 for all elements; *InhR*: inhalation rate, in this study, 20 m^3/day; *PEF*: particle emission factor, in this study, 1.36×10^9 m^3/kg.

Non-cancer risk is represented in terms of hazard index (*HI*) for multiple substances and/or exposure pathways. Hazard index (*HI*) and carcinogenic risk can be estimated using Eqs. (7-8), (USEPA, 1989):

$$HI = \sum \frac{ADD\ (or\ exposure\ \ intake)}{RfD\,(reference\ \ dose\,)} \tag{7}$$

$$Cancer\ Risk = LADD \times SF\,(slope\ \ factor) \tag{8}$$

3. Results and discussion

3.1. Descriptive statistical analysis

Descriptive statistics of heavy metal concentrations of topsoil at the two scales are presented in Table 1. The results show that mean concentrations of all heavy metals at those scales were higher than their corresponding background values in Shenyang (Wu, 1986), except, at small scale, for As. Mean concentrations of As at small scale were at lower levels than its regional background values, suggesting that As had not been enriched by anthropogenic activities. The highest concentrations of all heavy metals at both scales were lower than their corresponding pollution thresholds in China, based on the Chinese Environmental Quality Standard for Soils (MEP, 1995), except As at large scale. At that scale, 27.5% of As concentrations exceeded corresponding pollution thresholds. Thus, further monitoring and protection measures are required to prevent additional enrichment of As at large scale.

Coefficient of variation (CV) values among six heavy metals were Pb(0.35) > As(0.26) > Zn(0.19) > Cu(0.17) > Ni(0.09) > Cr(0.07) at small scale, and Pb(0.51) > Cu(0.32) > As(0.31) = Zn(0.31) > Ni(0.22) > Cr(0.19) at large scale. All CV values of the metals at large scale were larger than those at small scale. The greater CV values at large scale reflected stronger spatial variability. High concentrations coupled with the relatively high CV values for metal elements demonstrate the anthropogenic contribution in the study area (Manta et al., 2002). The high CV values of Pb, Cu and Zn at both scales were probably enriched by human activities, revealing a non-homogeneous distribution. The high mean concentrations coupled with relatively low CV values of Ni and Cr make it difficult to determine the potential influence of human activities on these metals.

3.2. Multivariate statistical analysis

Correlation analyses furnish an effective way to reveal the complicated relationships among heavy metals in soil. Table 2 presents Pearson correlation coefficients and their significance levels. Cu exhibited significantly positive correlations ($r > 0.62$) with Pb, Zn, Ni, Cr and As ($p<0.01$) at small scale, and at large scale with Pb, Zn, Ni, Cr ($p<0.01$) and As ($p<0.05$). Ni showed high and significant positive correlations with Cr at both scales ($r=0.88^{**}$ for small scale and $r=0.83^{**}$ for large scale), indicating common influences for the two metals. The concentration of As at large scale showed no significant correlation with other heavy metals ($p<0.01$), implying that source of As might differ from other heavy metals. The Pb values showed weak positive correlation ($r<0.23$) with Ni at both scales, suggesting different sources.

Several studies have proved that the association of these metals with the components can be indicated by the anthropogenic influence or geogenic and pedogenic characteristics (Bloemen et al., 1995; Hanesch et al., 2001). For the small scale, two principal components explained 85% of total varianceAs show in Table 3, As, Cr, and Ni were categorized as the first principal component (PC1). explaining 66% of total variance. The second component (PC2) explained 19% of total variance, loaded by Cu, Pb, and Zn (Table 3).

Cu and As showed high values in one component, but were also represented in another component ($Cu_{PC1}=0.577$, $Cu_{PC2}=0.739$, $As_{PC1}=0.663$, $As_{PC2}=0.47$). This suggests that their distributions are affected by both PC1 and PC2. For the large scale, PC1, explaining 64% of total variance, was dominated by Cu, Zn, Ni and Cr. PC2, explaining 17% of that variance, showed positive factor loadings of Pb and As.

Table 1. Summary statistics of heavy metal concentrations (mg/kg) in topsoil

	Scales	*Range*	*Mean*	*S.D.*	*Kurtosis*	*Skewness*	*C.V.(%)*	*Background[a]*	*Limit[b]*
As	small	4.75-14.94	7.99	2.06	3.92	1.70	0.26	8.79	30
	Large	10.20-38.60	24.06	7.38	-0.80	0.01	0.31		
Cr	small	78.70-102.50	91.26	6.28	-0.94	0.29	0.07	57.66	300
	large	50.60-122.90	83.77	15.79	0.35	0.35	0.19		
Cu	small	24.13-51.87	36.76	6.10	-0.16	0.32	0.17	24.57	100
	large	16.50-65.20	34.11	10.85	0.98	1.1	0.32		
Ni	small	30.46-44.04	37.98	3.45	-0.77	0.26	0.09	27.92	50
	large	15.90-46.00	32.51	7.20	-0.04	-0.13	0.22		
Pb	small	17.30-77.50	33.33	11.82	3.60	1.45	0.35	22.15	300
	large	17.70-114.50	46.38	23.78	1.66	1.4	0.51		
Zn	small	68.30-146.20	100.06	19.27	-0.61	0.31	0.19	59.84	250
	large	52.70-164.80	82.44	25.63	2.62	1.64	0.31		

Note: [a]Background value in Shenyang (Wu, 1986); [b]Chinese Environmental Quality Standard for Soils (State Environmental Protection Administration of China, 1995); S.D. is standard deviation; C.V. is coefficient of variation.

Table 2. Correlation matrix between heavy metal contents in study area

	Cu	*Pb*	*Zn*	*Ni*	*Cr*	*As*
The small scale						
Cu	1.00					
Pb	0.65**	1.00				
Zn	0.87**	0.76**	1.00			
Ni	0.73**	0.27*	0.46**	1.00		
Cr	0.60**	0.26	0.39**	0.88**	1.00	
As	0.62**	0.49**	0.55**	0.69**	0.56**	1.00
The large scale						
Cu	1.00					
Pb	0.75**	1.00				
Zn	0.88**	0.79**	1.00			
Ni	0.72**	0.23	0.43**	1.00		
Cr	0.88**	0.52**	0.74**	0.83**	1.00	
As	0.30*	0.24	0.26	0.18	0.11	1.00

*Note: *Significant correlation at level p< 0.05; **Significant correlation at level p< 0.01.*

Table 3. Total variance explained and rotated component matrix (two principal components selected) for heavy metal contents

Initial eigenvalues			***Element***	***Rotated component matrix***	
Total	***% of variance***	***Cumulative %***		***PC1***	***PC2***
Total variance explained				***Component matrixes***	
The small scale					
3.953	65.890	65.890	Cu	0.577	**0.739**
1.169	19.476	85.366	Pb	0.081	**0.920**
0.439	7.314	92.680	Zn	0.284	**0.905**
0.283	4.723	97.403	Ni	**0.954**	0.209
0.113	1.882	99.285	Cr	**0.926**	0.131
0.043	0.715	100.000	As	**0.663**	0.470
The large scale					
3.829	63.822	63.822	Cu	0.**848**	0.497
1.017	16.956	80.778	Pb	0.457	**0.723**
0.855	14.244	95.021	Zn	**0.675**	0.618
0.193	3.211	98.233	Ni	**0.883**	-0.042
0.068	1.134	99.367	Cr	**0.959**	0.165
0.038	0.633	100.000	As	-0.680	**0.760**

3.3. Geostatistical analysis

The semivariograms and fitted models for metals at different scales are given in Table 4. The nugget (C0) can be used to describe the spatial heterogeneity of intrinsic factors. The sill (C0+C) is considered the spatial heterogeneity of extrinsic factors. The ratio of nugget and sill (C0/C0+C), expressed as a percentage, is useful to classify spatial dependence. A ratio less than 25% indicates strong dependence, between 25% and 75% moderate, and greater than 75% weak (Cambardella et al., 1993). The range represents the distances beyond which observations are not spatially dependent (Sun et al., 2003). Values of the coefficient of determination (R^2) were significant at the 0.01 level via an F-test, indicating that the theoretical model reflected the spatial pattern of soil heavy metals. At large scale, the experimental semivariogram of those metals can be fit with a Gaussian model for Cu and Pb, a spherical model for Zn and Cr, an exponential model for Ni, and a linear model for As. The nugget/sill ratio of Cu was less than 25%, suggesting strong spatial dependence, whereas other metals showed moderate dependence. At small scales, semivariograms showed that Ni and As were all fit by the Gaussian model; the other four heavy metals were fit by the exponential model. The nug/sill ratios of Cu, Pb and Zn were between 1.42% and 19.64%, suggesting strong spatial dependence, whereas Ni, Cr and As showed moderate dependence. All sampling distances of soil heavy metals were within the ranges at both scales, demonstrating the rationality of the survey.

3.4. Spatial distribution

In this study, IDW was used to display the overall trend of soil heavy metal because of its advantages in pollution prediction (Xie et al., 2011). To compare the spatial distribution of heavy metals on both scales, the interval of interpolation was unified to estimate values in unsampled areas. The main factor affecting the accuracy of inverse distance interpolator is the parameter of power. In this study, we compared estimates of inverse distance interpolator using different power values 1, 2, 3 and 4, which are the most commonly used. It is found that the greater the weighting power, the large the hotspot area estimated by IDW. In this study, we choose 2 as the value of power parameter.

Table 4. Best-fit semivariogram models of heavy metals.

	Model	Nugget (C_0)	Sill (C_0+C)	C/(C_0+C)	Range(m)	R^2
The small scale						
Cu	Exponential	0.0077	0.15640	4.92%	816	0.759**
Pb	Exponential	0.00027	0.01904	1.42%	387	0.745**
Zn	Exponential	71.100	362.100	19.64%	903	0.732**
Ni	Gaussian	0.00971	0.03872	25.08%	681	0.771**
Cr	Exponential	0.00039	0.00077	50.65%	537	0.768**
As	Gaussian	0.01825	0.03840	47.53%	798	0.857**
The large scale						
Cu	Gaussian	0.01088	0.21860	4.978%	10946	0.900**
Pb	Gaussian	0.01863	0.04126	45.15%	5924	0.872**
Zn	Spherical	0.1890	0.630	30.00%	9920	0.730**
Ni	Exponential	33.100	97.300	34.02%	68760	0.814**
Cr	Spherical	137.900	275.900	49.98%	11260	0.775**
As	Linear	33.0384	63.0342	52.41%	11617	0.704**

*Note: **Significance at level p< 0.01.*

At large scale, estimated maps of six heavy metals concentrations in soil are presented in Fig. 2. Among these metals, the spatial distributions of Cr, Ni and Cu are remarkably similar over a large area, and have good correlation with river shapes. High levels of Pb and Zn around the Tiexi industrial district were likely caused by metals released in association with human activity. The spatial distribution of Pb showed low heterogeneity, in contrast to the other metals. This suggests that its concentrations may be from non-point source pollution, such as industrial fumes and coal burning exhaust, which can travel long distances. In contrast to Pb and Zn, the spatial distribution of As does not show this trend, and there were no clear hotspots.

At small scale, we identified the same several hotspots of high metal concentration in the interpolated maps of Cr, Ni, Cu, Pb and Zn. This suggests that the high concentration of these heavy metals may originate from the same process, either anthropogenic or natural. The dominant pollution pattern at small scale has more pollution hotspots and more apparently heterogeneous point pollution than at large scale, except for As. In general, more information can be gleaned from the interpolation map of small scale.

3.5. Exposure and risk assessment

The results of the risk assessment are shown in Table 5. The reference values (RfD) used in the analysis were taken from the US Department of Energy's RAIS compilation (USDE, 2004). The toxicity values for Pb have been taken from the WHO's Guidelines for Drinking Water Quality (WHO, 2008). As was considered non-cancer risk through ingestion and dermal. Inhalation-specific toxicity data are available only for Cr and Ni.

For the other three elements included in the risk analysis, the toxicity values considered for the inhalation route are the corresponding oral reference dose and slope factors, on the assumption that, after inhalation, the absorption of the particle-bound toxicants will result in similar health effects as if the particles had been ingested.

At two scales, the non-carcinogenic hazard index for all five heavy metals are much smaller than 1, indicating no potential non-carcinogenic risk for adults and children. The HIS for Cu, Pb, Zn, Ni, Cr and As to adults and children decrease in the order of Cr>Pb>Ni>Cu>Zn>As at small scale, while Cr>Pb>Ni>Cu>As>Zn at large scale. Compared to adult, children health index is larger, and their cumulative effect is also of concern for children.

At the two different scales, for cancer risk, the only carcinogen risk for inhalation exposure modes was considered in the model. The level of cancer risk associated with exposure to Ni and Cr falls within the range of threshold values (10^{-4}-10^{-6}) above which environmental and regulatory agencies consider the risk unacceptable.

4. Conclusions

This study analyzed the sources and spatial patterns of six soil heavy metals in Shenyang via statistical, geostatistical and spatial analyses, for understanding human and natural effects on these metals at two scales. Soil in the study region could be considered lightly or partially polluted by heavy metals. This is because average values of those metals at both scales were greater than corresponding background values, but less than guidance values for acid soil in China.

The major sources and spatial heterogeneity of heavy metals at two different scales did not always coincide in terms of spatial variation. Sampling scales have been showed effect for sources identification of heavy metals based on correlation analysis and principal component analysis. Thus, sampling scales should be considered when developing control measures for soil pollution.

The level of cancer risk in some sampling sites associated with exposure to Ni and Cr falls within the range of threshold values consider the risk unacceptable.

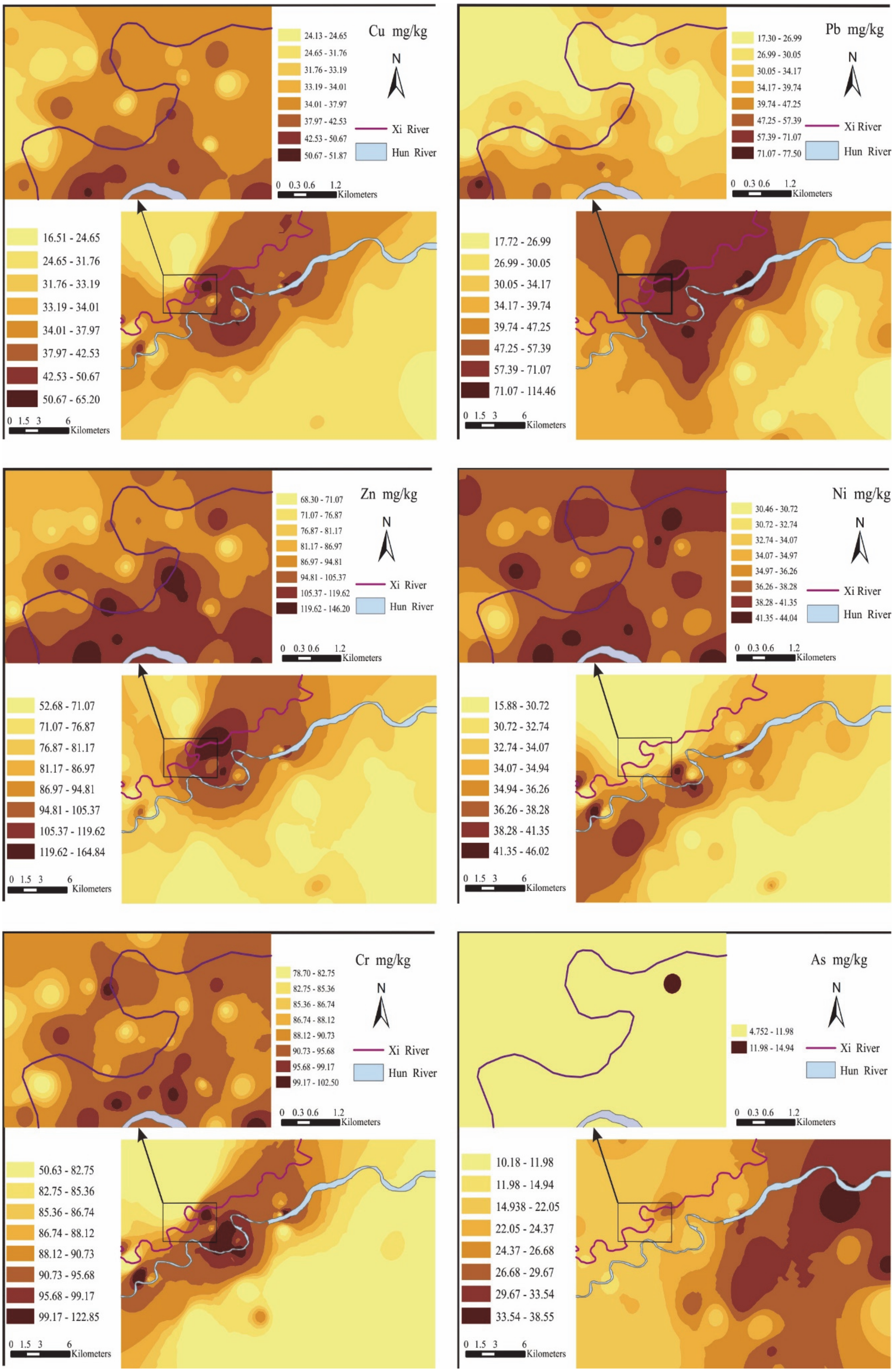

Fig. 2. Spatial distributions of soil Cu, Pb, Zn, Ni, Cr and As at two scales

Table 5. Hazard quotient and risk for each element and exposure pathway

Element	*C(95%UCL)*	*Oral RfD*	*Dermal RfD*	*Inhal .RfD*	*Inhal.SF*	HI_{chi}	HI_{adl}	*Cancer Risk*
The small scale								
Cu	38.71	0.04	1.20E-02	0.04		1.61E-03	8.26E-04	
Pb	37.11	3.50E-03	5.25E-04	3.50E-03		1.78E-02	9.38E-03	
Zn	106.22	0.30	0.06	0.30		5.90E-04	3.08E-04	
Ni	39.09	0.02	5.40E-03	2.06E-02	0.84	3.25E-03	1.67E-03	7.94E-09
Cr	93.27	3.00E-03	6.00E-05	2.86E-05	42.00	5.87E-02	4.05E-02	9.47E-07
As	8.65	3.00E-04	1.23E-04		15.10	3.41E-04	1.71E-04	3.16E-08
The large scale								
Cu	37.59	0.04	1.20E-02	0.04		1.56E-03	8.02E-04	
Pb	53.99	3.50E-03	5.25E-04	3.50E-03		2.58E-02	1.36E-02	
Zn	90.63	0.30	0.06	0.30		5.04E-04	2.62E-04	
Ni	34.81	0.02	5.40E-03	2.06E-02	0.84	2.89E-03	1.49E-03	7.07E-09
Cr	88.83	3.00E-03	6.00E-05	2.86E-05	42.00	5.59E-02	3.86E-02	9.02E-07
As	26.42	3.00E-04	1.23E-04		15.10	1.04E-03	5.21E-04	9.64E-08

Note: Oral RfD is the ingestion chronic reference values; Dermal RfD is chronic dermal reference values; Inhal .RfD is the inhalation chronic reference values; Inhal.SF is slope factor; HI_{chi} is hazard index of children; HI_{adl} is hazard index of adults.

The potential health impact of high levels of heavy metals on residents in nearby areas should be taken into consideration. Further investigation of heavy metal speciation and its bioavailability is required to reduce its pollution in the study area.

Acknowledgements
This study was financially supported by National Natural Science Foundation of China (No. 41807344). The authors would like to thank the Shenyang Institute of Geology and Mineral Resources.

References

Bloemen M.L., Markert B., Lieth H., (1995), The distribution of Cd, Cu, Pb and Zn in topsoils of Osnabrück in relation to land use, *Science of the Total Environment*, **166**, 137-148.

Cambardella C.A., Moorman T.B., Parkin T.B., Karlen D.L., Novak J.M., Turco R.F., (1993), Field-scale variability of soil properties in central lowa soils, *Soil Science Society of America Journal*, **58**, 1501-1511.

Camobreco V.J., Richards B.K., Steenhuis T.S., Peverly J.H., McBride M.B., (1996), Movement of heavy metals through undisturbed and homogenized soil columns, *Soil Science*, **161**, 740-750.

Chen T., Liu X.M., Li X., Zhao K.L., Zhang J.B., Xu J.M., (2009), Heavy metal sources identification and sampling uncertainty analysis in a field-scale vegetable soil of Hangzhou, China, *Environmental Pollution*, **157**, 1003-1010.

Chen T.B., Wong J.W.C., Zhou H.Y., Wong M.H., (1997), Assessment of trace metal distribution and contamination in surface soils of Hong Kong, *Environmental Pollution*, **96**, 61-68.

Cyrys J., Stölzel M., Heinrich J., Kreyling W.G., Menzel N., Wittmaack K., (2003), Elemetal composition and sources of fine and ultrafine ambient particles in Erfurt, Germany, *Science of the Total Environment*, **305**, 143-156.

Fu S., Wei C.Y., (2012), Multivariate and spatial analysis of heavy metal sources and variations in a large old antimony mine, China, *Journal of Soils and Sediments*, **13**, 106-116.

Gray C., McLaren R., Roberts A., (2003), Atmospheric accessions of heavy metals to some New Zealand pastoral soils, *Science of the Total Environment*, **305**, 105-115.

Hanesch M., Scholger R., Dekkers M.J., (2001), The application of fuzzy C-means cluster analysis and non-linear mapping to a soil data set for the detection of polluted sites, *Physics and Chemistry of the Earth*, **26**, 885-891.

Huang S.S., Liao Q.L., Hua M., Wu X.M., Bi K.S., Yan C.Y., (2007), Survey of heavy metal pollution and assessment of agricultural soil in Yangzhong district, Jiangsu Province, China, *Chemosphere*, **67**, 2148-2155.

Huo X.N., Li H., Zhang W.W., Sun D.F., Zhou L.D., Li B.G., (2009), Multi-scale spatial structure of heavy metals in Beijing cultivated soils, *Transactions of the Chinese Society of Agricultural Engineering*, **25**, 223-229.

Li X., Liu L., Wang Y., Luo G., Chen X., Yang X., (2013), Heavy metal contamination of urban soil in an old industrial city (Shenyang) in Northeast China, *Geoderma*, **192**, 50-58.

Li J.C., Liu Y., Yang Y.G., Qin Z.D., (2017), Characterization of soil heavy metal contamination and potential ecological risk in the urban-rural transition zone of Taiyuan City, China, *Environmental Engineering and Management Journal*, **16**, 413-420.

Lin Y.P., Cheng B.Y., Shyu G.S., Chang T.K., (2010), Combining a finite mixture distribution model with indicator kriging to delineate and map the spatial patterns of soil heavy metal pollution in Chunghua County, central Taiwan, *Environmental Pollution*, **158**, 235-244.

Liu Q., Sun J.K., Chen Y.P., Xia J.B., (2009), Spatial variability of the soil heavy metal with different sampling scales, *Chinese Journal of Soil Science*, **40**, 1406-1410.

Liu X., Wu J., Xu J., (2006), Characterizing the risk assessment of heavy metals and sampling uncertainty analysis in paddy field by geostatistics and GIS, *Environmental Pollution*, **141**, 257-264.

Manta D.S., Angelone M., Bellanca A., Neri R., Sprovieri M., (2002), Heavy metals in urban soils: a case study from the city of Palermo (Sicily), Italy, *Science of the Total Environment*, **300**, 229-243.

Matache M.L., David I.G., Dinu C., Radu L.G., (2018), Trace metals in water and sediments of the Prut river, Romania, *Environmental Engineering and Management Journal*, **17**, 1363-1371.

MEP, (1995), Chinese Environmental Quality Standard for Soils, (GB 15618-1955), State Environmental

Protection Administration of China, On line at: http://kjs.mep.gov.cn/hjbhbz/bzwb/trhj/trhjzlbz/199603/W020070313485587994018.pdf.

McGrath D., Zhang C., Carton O.T., (2004), Geostatistical analyses and hazard assessment on soil lead in Silvermines area, Ireland, *Environmental Pollution*, **127**, 239-248.

Pal S.K., Wallis S.G., Arthur S., (2018), An assessment of heavy metals pollution potential of road sediment derived from a suburban road network under different weather conditions, *Environmental Engineering and Management Journal*, **17**, 1955-1966.

Richards B.K., Steenhuis T.S., Peverly J.H., McBride M.B., (1998), Metal mobility at an old, heavily loaded sludge application site, *Environmental Pollution*, **99**, 365-377.

Saito H., Goovaerts P., (2000), Geostatistical interpolation of positively skewed and censored data in a dioxin-contaminated site, *Environmental Science & Technology*, **60**, 1237-1247.

Semenzin E., Critto A., Carlon C., Rutgers M., Marcomini A., (2007), Development of a site-specific Ecological Risk Assessment for contaminated sites: part II. A multi-criteria based system for the selection of bioavailability assessment tools, *Science of the Total Environment*, **379**, 34-45.

Sun B., Zhou S., Zhao Q., (2003), Evaluation of spatial and temporal changes of soil quality based on geostatistical analysis in the hill region of subtropical China, *Geoderma*, **115**, 85-99.

Sun Y., Zhou Q., Xie X., Liu R., (2010), Spatial, sources and risk assessment of heavy metal contamination of urban soils in typical regions of Shenyang, China, *Journal of Hazardous Materials*, **174**, 455-462.

Sylla M., Stein A., Breemen N., Fresco L.O., (1995), Spatial variability of soil salinity at different scales in the mangrove rice agro-ecosystem in West Africa, *Agriculture, Ecosystems and Environment*, **54**, 1-15.

Tomczak M., (1998), Spatial Interpolation and its uncertainty using automated anisotropic inverse Distance Weighting (IDW)-Cross-Validation/Jackknife approach, *Journal of Geographic Information and Decision Analysis*, **2**, 18-30.

USDE, (2004), RAIS: Risk Assessment Information System, U.S. Department of Energy, On line at: http://risk.lsd.ornl.gov/rap_hp.shtml.

USEPA, (1989), Risk assessment guidance for superfund, EPA/540/1-89/002, Washington, DC: Environmental Protection Agency, Office of Superfund Remediation and Technology innovation Environmental Protection Agency, On line at: http://www.epa.gov/oswer/riskassessment/ragsf/.

USEPA, (1997), Exposure factors handbook, EPA/600/P-95/002F, Washington, DC: Environmental Protection Agency, Office of Research and Development, On line at: http://www.epa.gov/superfund/resources/soil/toc.htm#p1.

USEPA, (2001), Supplemental guidance for developing soil screening levels for Superfund sites, OSWER 9355.4-24, Washington, D.C: Office of Solid Waste and Emergency Response, On line at: http://www.epa.gov/superfund/resources/soil/ssgmarch01.pdf.

Vrščaj B., Poggio L., Marsan F.A., (2008), A method for soil environmental quality evaluation for management and planning in urban areas, *Landscape and Urban Planning*, **88**, 81-94.

Wei B., Yang L., (2010), A review of heavy metal contaminations in urban soils, urban road dusts and agricultural soils from China, *Microchemical Journal*, **94**, 99-107.

WHO, (2008), Guidelines for drinking-water quality, incorporating first and second addenda to third edition, Vol. 1, Recommendations, World Health Organization, Geneva, On line at: http://www.who.int/water_sanitation_health/dwq/gdwq3rev/en/.

Wu Y.Y., (1986), Soil environmental background values in Shenyang, (in Chinese), *Environmental Protection Science*, **4**, 24-28.

Xie Y., Chen T.B., Lei M., Yang J., Guo Q.J., Song B., (2011), Spatial distribution of soil heavy metal pollution estimated by different interpolation methods: accuracy and uncertainty analysis, *Chemosphere*, **82**, 468-476.

Yu R.L., Xu J.Q., Hu G.R., (2017), Application of fly ash-stabilized municipal sewage sludge on growth of brassica chinensis and heavy metal transfer in pot experiment with a barren soil, *Environmental Engineering and Management Journal*, **16**, 2803-2812.